Effect of Tempering Treatment on Microstructure and Mechanical Properties of the HSLA-100 Steel

M. P. Dabir [1], H. Saffari [2], A. Kermanpur *[3]

Department of Materials Engineering, Isfahan University of Technology, Isfahan, Iran

Abstract

The high strength low alloy (HSLA) 100 steel has been widely used in various industries such as shipbuilding, military, oil and gas. An increase in yield strength with a reasonable toughness is highly demanding in this steel. In the present study, the quench-tempering heat treatment was investigated to improve mechanical properties of this steel. The samples were austenitized at 930 °C for 1 h followed by water quenching. They were then tempered in the temperature range of 410 and 710 °C for 1 to 4 h. Microstructures of the heat treated specimens were evaluated by optical and scanning electron microscopy, while mechanical properties measured by hardness, tensile, and toughness tests. The results showed that microstructural changes during tempering took place mainly after 650 °C, where the martensite laths and acicular ferrite transformed to polygonal ferrite. The yield and ultimate strengths were increased by increasing tempering temperature from 410 to 525 °C, beyond which both was dropped up to 710 °C. The maximum yield and ultimate strengths were obtained by tempering at either 525 °C for 1 h or 475 °C for 2 h. Increasing tempering temperature and duration both resulted in an increase in the absorbed impact energy.

Keywords:HSLA 100 steel; Tempering heat treatment; Mechanical properties; Fractography.

1. Introduction

It is more than three decades that low-alloy high-strength (HSLA) steels are interested by industries and researchers. HSLA 100 steel is one of this steel group which has been widely used after the second world war. Its range of applications has further more than shipbuilding and structures; nowadays, it is used in nuclear power plants, oil and gas piping, and military applications[1-4]. The chemical composition of the steel has designed to increase strength and toughness and to improve weldability. Titanium, copper, chromium, nickel, vanadium, and niobium are the main alloying elements. The presence of copper and its precipitates is intended to increase toughness in addition to strength[5-9]. On the other hand, the presence of nickel and chromium also increase hardenability and strength. This improvement can only be achieved by using desirable heat treatment[10]. In addition, the formation of complex precipitates is another approach to increase strength of these quenched steels. This has been studied in depth by Mishra et al. in 2002[11].

Many researches have been done so far in order to obtain optimum properties in HSLA 100 steel. The variation of microstructure and increasing strength and thickness by using different heat treatment have been

*Corresponding author
Email: ahmad_k@iut.ac.ir
Address: Department of Materials Engineering,
Isfahan University of Technology, Isfahan,
P.O. Box: 84156-83111 Iran
1. Undergraduate
2. M.Sc.
3. Professor

the intention of the researchers [2,8,12-15]. The ultimate microstructure after the heat treatment has shown great importance to change their mechanical properties. Achieving a tough microstructure while maintaining strength has been considered. Also, higher impact energy at low temperatures has been intended especially for high-strength low-temperature applications[16]. Several methods exist for optimizing these parameters. These are such as the neural network, simulation software, and design and experiment. Wilson et al.[8] have investigated variation of mechanical properties by aging temperature. They reported the probable structures by considering the temperature-time plots during continuous cooling. Rey et al.[7] developed a model of strength and toughness. It has been revealed that temperature and time of austenitizing, cooling rate, and time and temperature of aging are the main factors in the heat treatment of HSLA steels. Variation of these parameters could affect mechanical properties such as yield strength, ultimate tensile strength, absorbed impact energy and hardness. Recently, the application of thermomechanical processing[17], multistage heat treatment [12] and single-stage heat treatment has been investigated.

In spite of numerous studies on the heat treatment of HSLA steels, challenges still exist. In fact, different optimum heat treatment conditions have been reported due to the various perspectives and experimental conditions [16-20]. The purpose for this study is to evaluate the effects of temperature and duration of tempering heat treatment on yield strength, ultimate strength, and toughness considering low temperature tempering conditions. The best tempering conditions were reported with respect to the achieved mechanical properties.

2. Materials and Experimental Procedures

In this study, HSLA 100 steel was used and its chemical composition was evaluated by optical emission spectrometry (OES) according to ASTM E1507-07 (Table 1). A steel plate of 12×200×100 mm^3 was adopted. The heat treatment was conducted using a Carbolite electric furnace. The quench-tempering heat treatment at a constant austenitizing temperature of 930 °C was carried out at a temperature range of 410 to 710 °C, and a temperature of 475 °C at three times of 1, 2, and 4 hours. Also, the effect of sub-zero treatment (quenching in liquid nitrogen) before tempering was studied by taking into account a separate heat treatment. The details and designations of the performed heat treatments are presented in Table 2. For each heat treatment cycle, relative to the test design, three tensile samples were applied according to ASTM E8 with dimensions presented in Fig. 1a. In order to study the impact energy of the heat-treated samples, according to ASTM E23b, Charpy impact samples with dimensions according to Fig.1b were extracted and tested at -20 °C by Welestor equipment. In order to study hardness changes, Rockwell hardness test was carried out using automatic machine model Copa UV1. The optical microscopy images were obtained from the samples grinded with 80 to 2400 sandpapers, polished with 1 µm alumina powder, and etched with 2% Nital solution. For more precise studies on fracture surfaces and microstructure, scanning electron microscopy (SEM Philips XI30) was adopted. Characterization of the precipitates inside the microstructure was conducted by energy-dispersive X-ray spectroscopy. For theoretical studies on carbon equivalent values and critical temperatures, the equations present in literature[21-24] were used. These calculated values are listed in Table 3.

Table 1. The measured (by OES[25]) and standard chemical composition of HSLA 100 (wt%).

Element	Fe	S	P	Nb	Si	Cu	Mn	C	Al	Mo	Ni	Cr
Measured	Balance	0.009	0.012	0.029	0.26	1.58	0.84	0.04	0.03	0.59	3.55	0.55
Standard	Balance	0.006	0.015	-	0.15-0.38	1.45-1.75	0.75-1.05	0.04-0.06	-	0.35-0.60	2.75-3.50	0.45-0.75

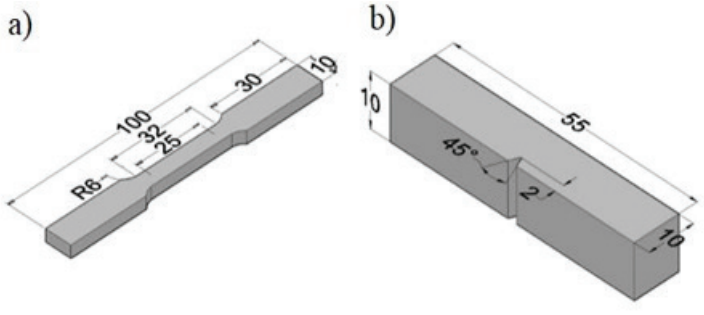

Fig. 1. (a) Schematic of the tensile sample and its dimensions according to ASTM E8, (b) Schematic of the impact sample and its dimensions according to ASTM E23b (in mm).

Table 2. Heat treatment cycles for various samples.

Sample Name	Austenitization		Cooling Environment	Tempering		Cooling Environment
	Temperature (C°)	Time (h)	*	Temperature (C°)	Time (h)	*
ASR	-	-	-	-	-	-
H_{4101}	930	1	W	410	1	W
H_{4751}	930	1	W	475	1	W
H_{5251}	930	1	W	525	1	W
H_{6501}	930	1	W	650	1	W
H_{7101}	930	1	W	710	1	W
H_{4752}	930	1	W	475	2	W
H_{4754}	930	1	W	475	4	W
HN_{4754}	930	1	W+N	475	4	W
*W (Water), N (Liquid Nitrogen).						

Table 3. Carbon equivalent, critical temperature, and temper-embrittlement susceptibility[21,23,24,26].

X	J	Bs	Ms	A_{c3}	A_{c1}	C_{Eq}
0.0012	104	523	432	845	670	0.79
C_E = C + Mn/6 + (Cr + Mo + V)/5 + (Ni + Cu)/15+ Si/6						
A_{c1}=723-10.7Mn-16.9Ni+29.1Si+16.9Cr+290As+6.38W						
A_{c3}=910-203√c-15.2Ni+44.7Si+104V+31.5Mo+13.1W						
M_s=512-453C-16.9Ni+15Cr-9.5Mo+217(C)2-71.5(C)(Mn)-67.6(C)(Cr)						
B_s=771-231.5C-69Mn-23Si-58.5Cr-31Ni-55Mo-41V						
J= (Mn + Si) (P + Sn) x10^4 (in wt %)						
X=(10P + 5Sb + 4Sn + As)/100 (in ppm)						
If J is less than or equal to 180, or if X is less than 20, the risk of temper embrittlement is considered to be low. A limit in this form can be specified for procurement, where concerns over temper embrittlement exist						

3. Results and Discussion

3.1. Microstructures

Previous investigations have shown that the microstructure of HSLA 100 steel is highly dependent on the performed heat treatment. The observed microstructures are a combination of low-carbon martensite, retained austenite, bainite, Widmanstätten ferrite, and ferrite according to their cooling rate[1)7)19)]. As shown in Fig. 2, microstructure of the H4754 sample included an acicular microstructure. For a more precise microstructural analysis, imaging by transmission electron microscopy is required. This method has not been used in the present study. However, the presence of an acicular structure is obvious in the microstructure. According to the Rockwell-C hardness results after quenching in water, it is possible that this structure is a low-carbon martensitic microstructure, or a combination of bainite and Widmanstätten ferrite. The width of the observed laths is between 3 to 8 μm, and their length is approximately between 5 to 50 μm with various distributions. Another point in Fig. 2 is the difference between the size of the formed laths. This, which comes from the grain size of the primary austenite grain, has resulted in recrystallization at some regions in the primary grains and also during re-austenitization. This can be a reason for the fine grains of the austenite at some regions[26)].

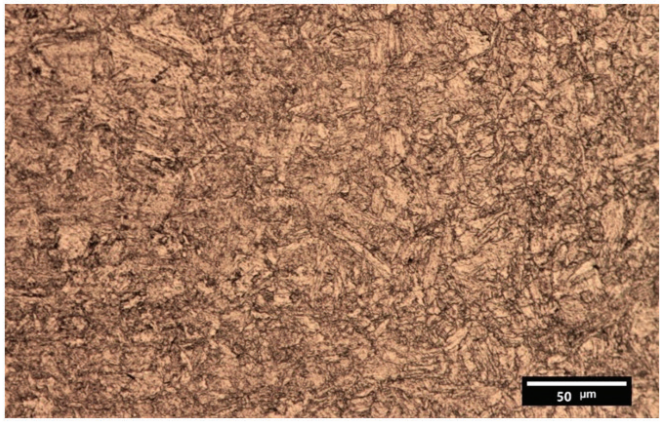

Fig. 2. Optical micrograph of H4754 heat-treated HSLA 100 specimen.

SEM investigations were carried out for more detailed microstructural studies. The obtained images from H4751 and H4754 samples are presented in Figs. 3a and 3b. In these images with higher resolution and magnification, the lath structure is clearly observed. Comparing Figs. 3a and 3b, it is observed that, as tempering time is increased, the large laths are decomposed to the finer ones. In addition, precipitation of the Cu-rich particles is also occurred [5,7,11,15,19,28], which cannot be detected by SEM investigation. It is reported that during tempering, carbon diffusion would take place and the low-carbon martensite is transformed to the acicular ferrite. The circularity of the lath tips is also increased by tempering, as shown in Figs. 3a and 3b.

The optical micrographs of the heat-treated samples, H4751, H5251, H6501, and H7101 are shown in Figs. 4a, 4b, 4c, and 4d, respectively. It can be observed that 1 h tempering from 475 °C to 650 °C does not include any noticeable structural changes due to the fact that temperature is below AC1. However, by a more survey look at the images, it can be observed that the sharpness of the laths is decreased by increasing tempering temperature and more ferritic regions are observed in the microstructures which are shown by white arrows in Fig. 4. It is expected to observe a decrease in the distortion and residual stress of the heat treated samples in spite of small microstructural changes. In the previous studies, it has been shown that temperature increase could decrease dislocation density[13]. Tempering at 710 °C has shown another microstructural feature as shown in Fig. 4d. It can be seen that most of the martensite laths and acicular ferrites have transformed to polygonal ferrites. This transformation would result in a great impact on mechanical properties which will be discussed later[4].

3.2. Mechanical Properties

In this study, tensile, impact, and hardness tests have been utilized in order to investigate the contributions of tempering temperature and duration on mechanical properties. All the results are presented in Table 4.

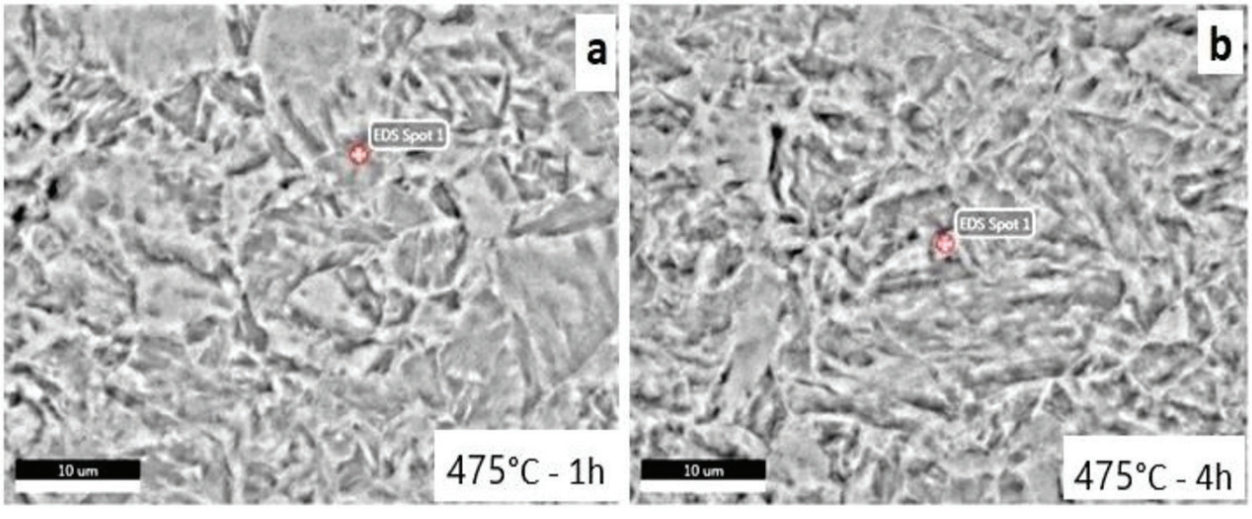

Fig. 3. SEM images of heat-treated samples at 475 °C for a duration of (a) 1 h (H4751) and (b) 4 h (H4754).

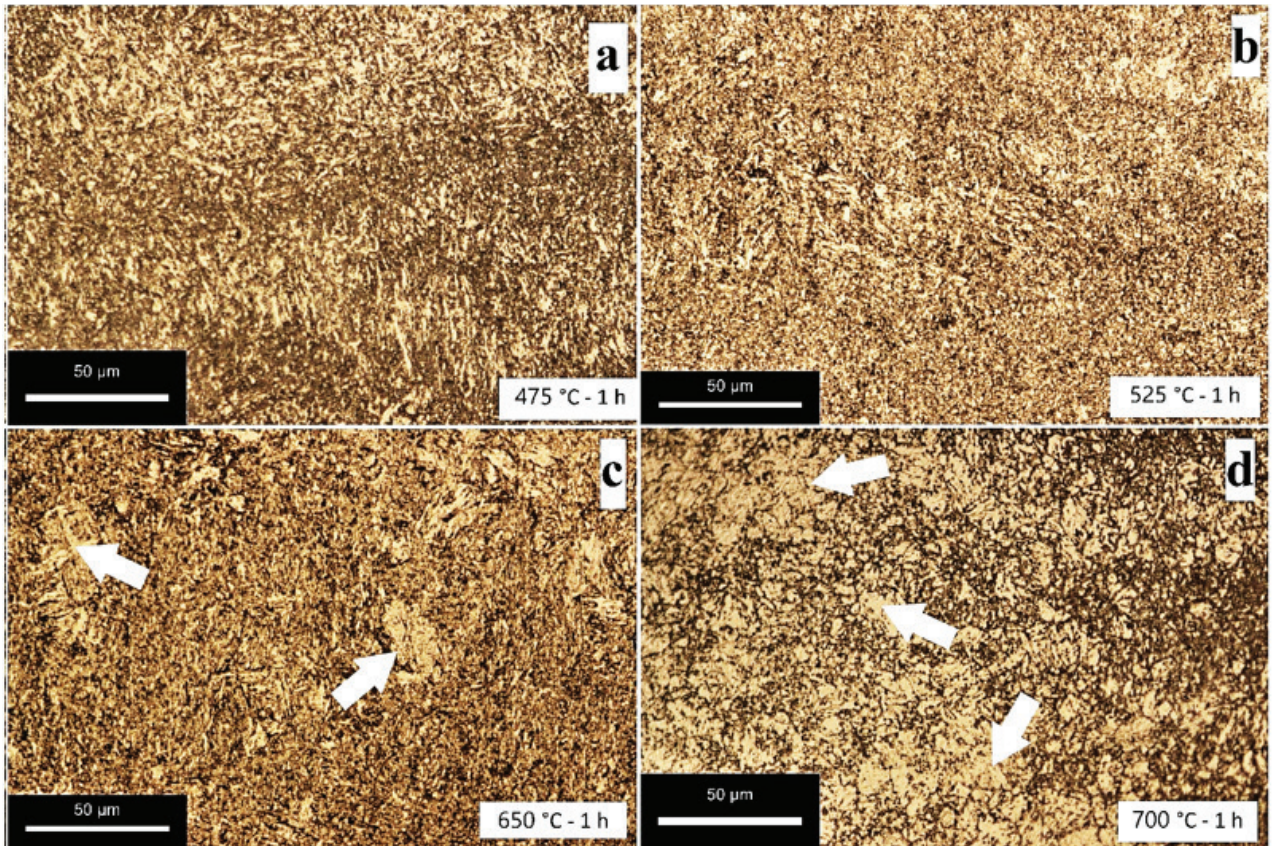

Fig. 4. Optical micrographs of tempered samples for 1 h at (a) 475 °C (H4751), (b) 525 °C (H5251), (c) 650 °C (H6501), and (d) 710 °C (H7101).

Table 4. Mechanical properties of all samples.

Sample	Hardness HRC	Yield Strength MPa	Tensile Strength MPa	Elongation %	Impact Energy J
H4101	36.6±0.6	895±11	956±8	10±0.6	33±5
H4751	32±1.4	980±12	990±5	15±0.8	41±4
H4752	34.5±1.7	1000±5	1025±9	11±1	67±2.5
H4754	35±1.1	970±10	978±8	16±0.5	88±2
H5251	35.5±0.5	990±7	1005±11	12.6±1	70±3.1
H6501	30.7±0.8	790±15	960±16	25±1.2	105±2.9
H7101	28.2±1	800±9	885±6	21±0.8	97±4.2
HN4754	36.1±1.5	1065±48	1085±13	13±1.7	90±2

The variation of yield strength, ultimate strength and elongation with temperature changes between 410 and 710 °C for 1 h is presented in Fig. 5. It is obvious that by increasing the temperature, the yield and ultimate strength values firstly increase and then decrease. This is in conformity with previous studies and is a result of strength increase by precipitation hardening[5]. When temperature increases to 450 °C, coherent micro-precipitates are formed. In addition, due to the formation kinetics of these precipitates, increasing temperature

would result in a higher amount of [27]. This increase is considerable up to 525 °C. However, a severe decrease in yield strength and especially ultimate strength is observed after 525 °C. This is expected to be the result of an increase in principates size due to their growth and becoming non-coherent with the matrix. Besides, temperature increase has additionally studied in some research works by using TEM. They have shown that dislocation forests have decreased and therefore, the locked dislocations have moved easily and this resulted in a reduction in strength. This has affected elongation; a decrease in elongation observed at 710 °C, which is due to the microstructural changes and phase transformations occurred close to AC1. This can be concluded according to the optical micrograph obtained as in Fig. 4d. Carbide formation and growth is one of the most effective parameters for the reduction in elongation at this temperature. The same results have been reported in the previous studies. Considering Figs. 4(b), 4(c) and 4(d), by increasing tempering temperature, the amount of depleted ferrite zones increased. Therefore, as going beyond AC1 temperature, this phenomenon was intensified and as a result, the ultimate strength and yield strength decreased.

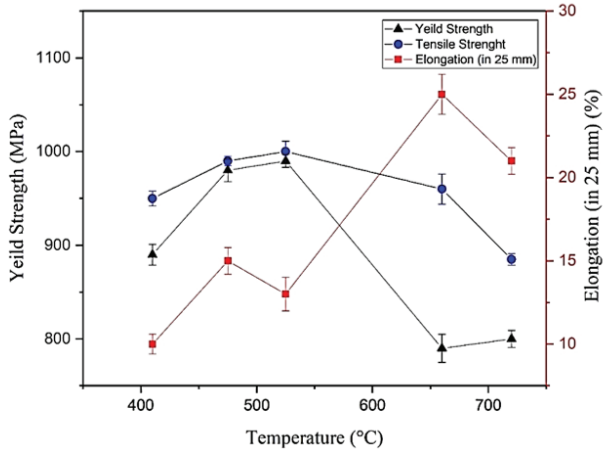

Fig. 5. Variation of the yield strength, ultimate strength, and elongation with tempering temperature for 1 h.

In Fig. 6, changes in hardness and impact energy by variation in tempering temperature from 420 to 710 °C have been plotted for a duration of 1 h. Hardness decreases by increasing temperature, considering tempering of the lath microstructure from the beginning to 475 °C. However, at 525 °C, the secondary hardness is the reason of hardness increasing. This hardness is due to the formation of fine copper precipitates and complex coherent precipitates which are referred to in the study performed by Das et al[29]. As temperature increases from 525 °C to the higher temperatures, a decrease in hardness is observed which is due to the over-aging of the formed precipitates. In addition to this, microstructural changes such as an increase in the ferrite zone and the disintegration of the lath microstructure may occur in this condition.

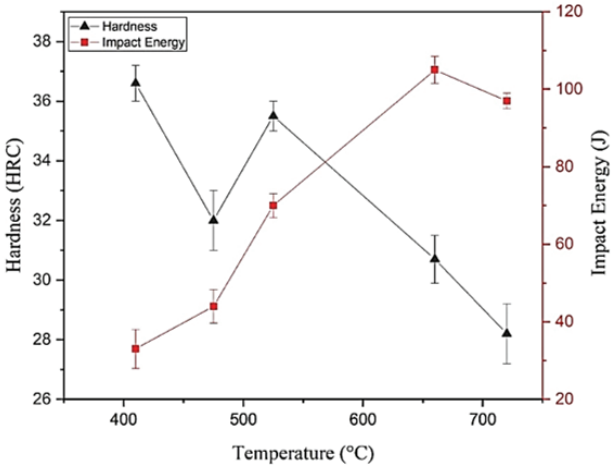

Fig. 6. Variation of the impact energy and hardness with tempering temperature for 1 h.

The changes in the impact energy versus tempering temperature for 1 h is observed in Fig. 6. The increase in tempering temperature has resulted in an increase in the impact energy. Considering the observed microstructures in Fig. 4, small changes in the microstructural features has occurred as temperature increased from 410 to 475 °C. However, the impact energy is increased which is believed to be due to more precipitation. The observed microstructures at 710 °C showed the formation of polygonal ferrites (Fig. 4) and carbide formation at the grain boundaries which leads to a reduction of impact energy. Additionally, the formation of austenitic islands is probable at the temperature close to AC1, where could transform to martensite during further rapid cooling. This could also affect the reduction of the impact energy.

The effect of tempering time on mechanical properties at 475 °C for three durations of 1, 2, and 4 h is plotted in Fig. 7. The results show that the yield and tensile strengths are firstly increased at the expense of elongation up to 2 h, beyond which a reverse trend is occurred for the mechanical properties. It is conceivable to assume that at the first period, coherent and complex copper precipitates are formed resulting in a higher strength and lower elongation. However, as the tempering is progressed, more diffusion would make precipitate growth, resulting in a higher precipitate size and possibly a change in the precipitate/matrix interface nature from coherent to non-coherent. This condition would cause a decrease in strength as shown in Fig. 7[30].

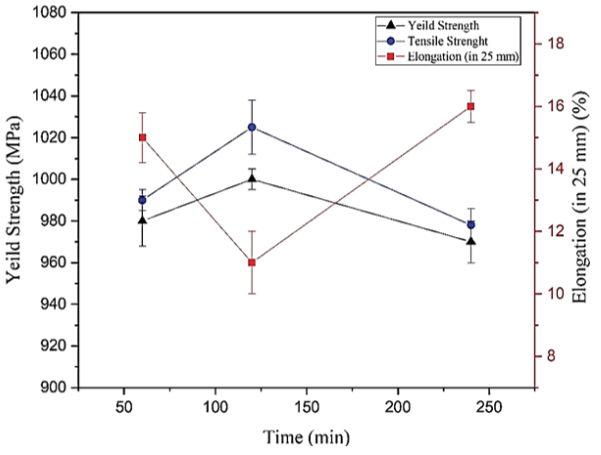

Fig. 7. Variation of yield strength, ultimate strength, and elongation with tempering duration at 475 °C.

Variations of hardness and impact energy against tempering duration are plotted in Fig. 8. The increase in tempering time from 1 to 2 h, and finally to 4 h at 475 °C has been accompanied with an increase in the impact energy. In fact, the impact energy is doubled after 4 h tempering at 475 °C. Interestingly, hardness is increased with time up to 2 h, beyond which it is unchanged. Although the strength has been reduced in the last stage of tempering, the occurrence of secondary hardening and formation of copper and complex precipitates would keep hardness unchanged[31],

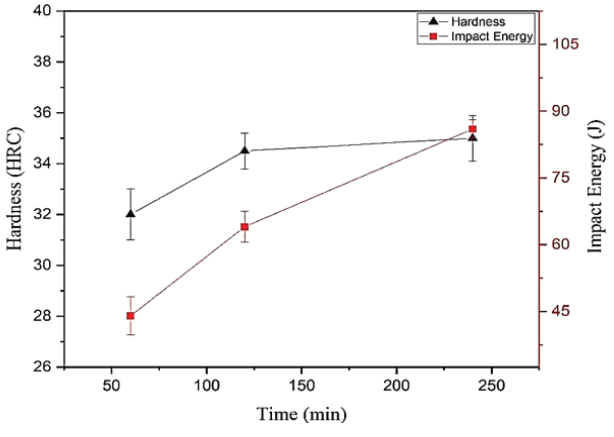

Fig. 8. Variation of the impact energy and hardness with tempering duration at 475 °C.

As shown in Table 1, the presence of 3.5 wt% nickel alloying element in this steel, in addition to the solid solution strengthening effect, might increase the volume fraction of the retained austenite. In order to investigate the effect of this retained austenite and its transformation to secondary martensite, a sub-zero process was conducted. The mechanical properties of the two samples of H4754 and HN4754 are presented in Table 4. The increase in the yield strength and the ultimate strength of the sub-zeroed HN4754 sample despite the same tempering conditions clearly show that the retained austenite has transformed to martensite and the sub-zero operation has been effective. This is also observable as an increase in hardness and a decrease in elongation of the sub-zero sample can be seen in comparison with the sample without sub-zero processing, although in some cases, the effect of this process has been negligible due to the amount of the retained austenite in the steel[32].

3.3.Fractography

The fracture surface of the samples tempered for 1 h at different temperatures is shown in Fig. 9. In Fig. 9a, many cleavage planes can be observed as an indicator of a brittle fracture. The EDS analyses related to the inclusions and remained precipitates on the fracture surfaces are shown in Figs. 10a and 10b. The high amount of niobium, aluminum, and titanium suggest that these particles could probably be niobium and titanium carbides as well as aluminum and titanium oxides[3]. These particles are the main source of dimple formation and crack origins in the microstructure. As observed in Fig. 9b, temperature increase has resulted in an increase in the semi-cleavage regions. These regions are accompanied by an increase in dimple number. At 525 °C, as copper precipitates may form, the number of the dimples are also increased (Fig. 9c). At the higher tempering temperature (650 °C), precipitate growth would occur which results in a coarser dimple size as shown in Fig. 9d. Therefore, it can be concluded that as tempering temperature is increased, the fracture type changes from cleavage (brittle) to semi-cleavage and finally to ductile fracture including dimples. This is in conformity with the changes in the absorbed impact energy, which have been obtained by impact test as shown in Fig. 6.

The effect of tempering time at 475 °C on the fracture surface type and its variation is observed in Fig. 11. The fracture is mainly brittle after 1 h tempering as shown in Fig. 11a. As time is increased from 1 to 2 h, fracture is generally ductile and mainly dimples form (Fig. 11b). Increasing the time to 4 h is accompanied with an increase in the diameter and depth of the dimples (Figs. 11c and 11d). The obtained results are in accordance with the results shown in Fig. 8. In addition, in some previous studies, these variations have been attributed to the formation and growth of copper and complex precipitates[7]. The EDS analysis shows that the remained particles at the end of the formed dimples contained high percentages of Ti and Al as respectively shown in Figs. 12a and 12b. It is possible that the Ti-containing particles are TiC-type and the Al-containing ones are oxides. The observed secondary particles are one of the main reasons for the formation of dimples.

Other parameters such as copper precipitates which were not detectable by SEM and were mentioned in other studies, could have contributions to the formation of dimples[32,3,7,33].

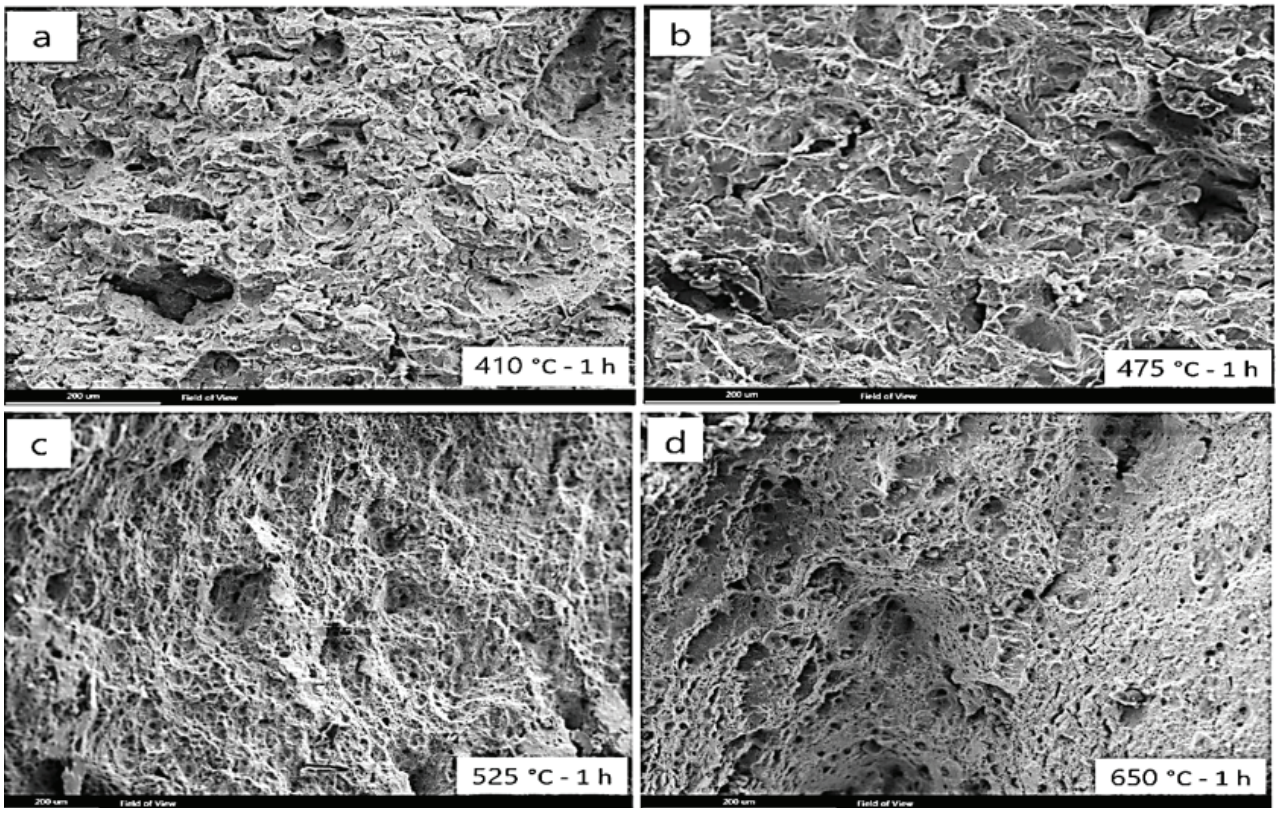

Fig. 9. SEM images of the fracture surface of the tempered samples for a duration of 1 h at (a) 410 °C (H4101), (b) 475 °C (H4751), (c) 525 °C (H5251), and (d) 650 °C (H6501).

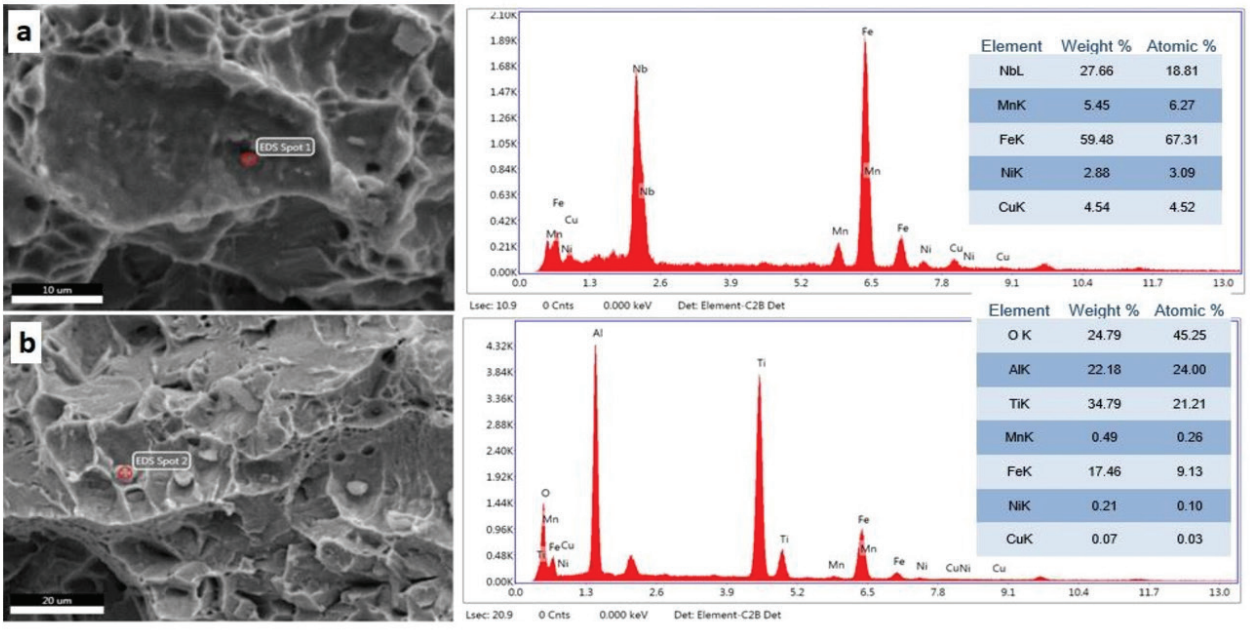

Fig. 10. EDS analysis of the particles on the fracture surface of H4101 sample suggesting (a) alloy carbides like NbC, and (b) oxides like TiO_2 and Al_2O_3.

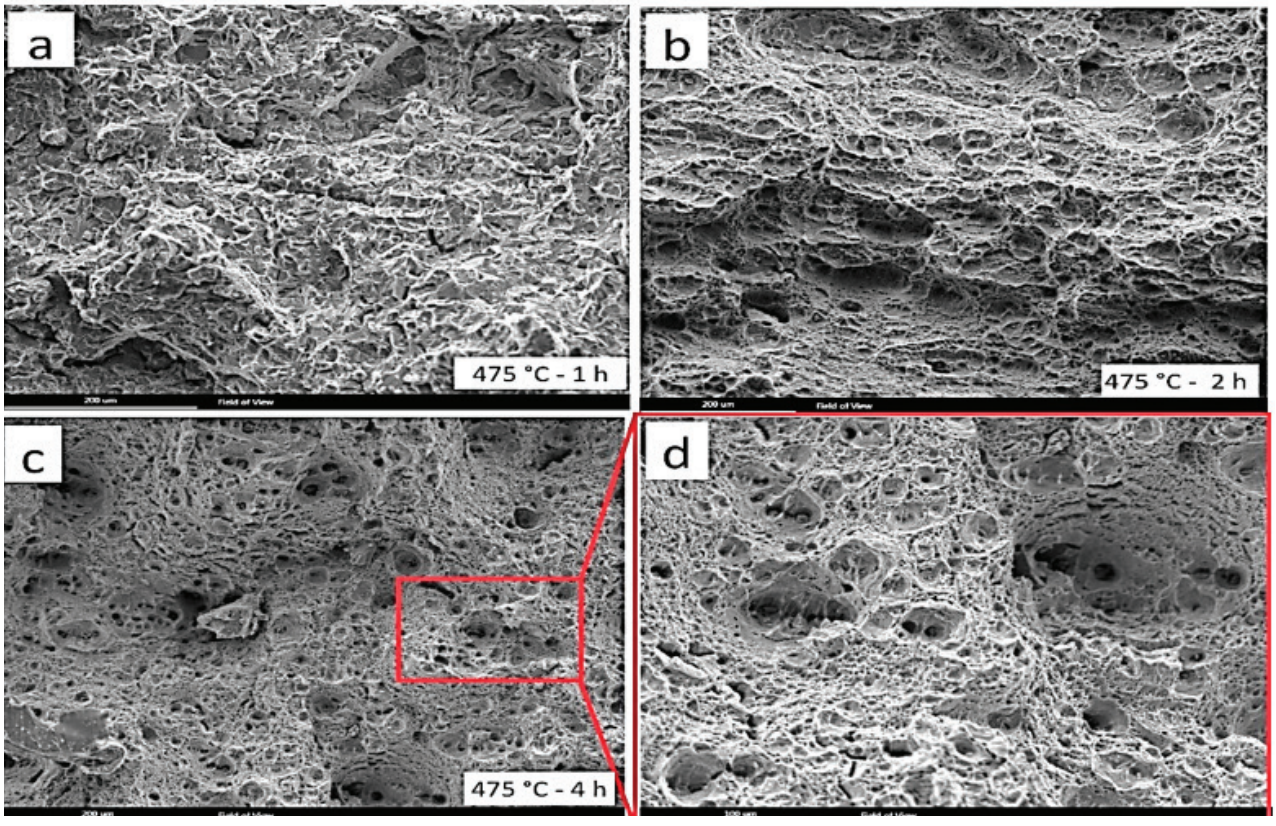

Fig. 11. SEM images of the fracture surface of the impact-test samples heat treated at 475 °C for (a) 1 h (H4751), (b) 2 h (H2754), and (c) 4 h (H4754).

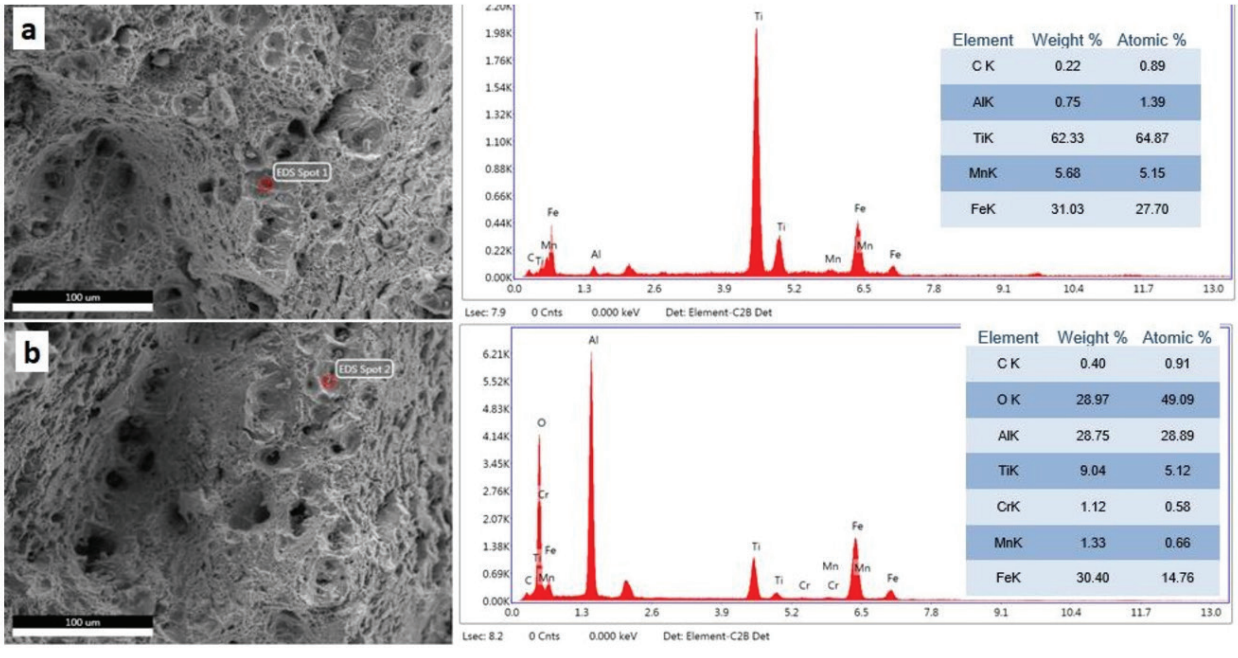

Fig. 12. EDS analysis of the particles on fracture surface of H4754 sample suggesting (a) TiC and (b) Al_2O_3 oxide particles.

4. Conclusions

The following conclusions can be obtained from the present work:

- The microstructure of the as-quenched HSLA 100 steel was mainly contained low-carbon martensite

and acicular ferrite.

- The yield and ultimate strengths were increased by increasing tempering temperature from 410 to 525 °C, beyond which both was dropped up to 710 °C.
- A secondary hardening was found by tempering at 525 °C for 1 h.
- The maximum yield and ultimate strengths were obtained by tempering at either 525 °C for 1 h or 475 °C for 2 h.
- Increasing tempering temperature and duration both resulted in an increase in the absorbed impact energy.
- A brittle fracture was occurred at 410 °C. However, the fracture behavior was changed to ductile with increasing tempering temperature.

Reference

[1] W. Yu, Y. Qian, , H. Wu, Y. Yang: J. Iron Steel Res. Int., 18 (2011) 64–69.

[2] S. K. Das, N. Narasaiah, S. Sivaprasad, S. Chatterjee, S. Tarafder: Mater. Sci. Technol., 23 (2007) 177–182.

[3] S.K. Das, S. Sivaprasad, S. Das, S. Chatterjee, S. Tarafder : Mater. Sci. Eng. A, 431 (2006) 68–79.

[4] S.K. Dhua, A. Ray, D.S. Sarma: Mater. Sci. Eng. A, 318 (2001) 197–210.

[5] J.E. Kim, J.-B. Seol, W.-M. Choi, B.-J. Lee, C.-G. Park : Met. Mater. Int., 24 (2018) 525–531.

[6] S. Ojha, N. S. Mishra, B. K. Jha : Bull. Mater. Sci., 38 (2015) 531–536.

[7] P. K. Ray, R. I. Ganguly, A. K. Panda : Mater. Sci. Eng. A, 346 (2003) 122–131.

[8] A. D. Wilson, E. G. Hamburg, D. J. Colvin, S. W. Thompson, G. Krauss : Microalloyed HSLA steels, (1988) 259–275.

[9] S. K. Dhua, D. Mukerjee, D. S. Sarma : Metal. Mater. Trans. A, 32 (2001) 2259–2270.

[10] R. P. Kolli, D. N. Seidman : Acta Mater., 56 (2008) 2073–2088.

[11] S. K. Mishra, S. Das, S. Ranganathan : Mater. Sci. Eng. A, 323 (2002) 285–292.

[12] Y. Liu et al. : Mater. Sci. Eng. A, 675 (2016) 371–378.

[13] M. Mujahid, A. K. Lis, C. I. Garcia, A. J. DeArdo : J. Mater. Eng. Perform., 7 (1998) 247–257.

[14] H. Güler, R. Ertan, R. Özcan : Mater. Test., 54 (2012) 619–624.

[15] M. Venkatraman, O. N. Mohanty, R. N. Ghosh : Scand. J. Metall., 30 (2001) 8–13.

[16] S. W. Thompson : Mater. Sci. Eng. A, 711 (2018) 424–433.

[17] M. Arumugam, P. R. Narayanan, V. Muthupandi : Met. Mater. Int., (2019) 1–10.

[18] S. H. M. Anijdan, M. Sabzi : in TMS Annual Meeting & Exhibition (Springer, 2018). 145–156.

[19] A. R. H. Far, S. H. M. Anijdan, S. M. Abbasi : Mater. Sci. Eng. A, 746 (2019) 384–393.

[20] W. A. Jadayil, D. Serhan : in TMS 2019 148th Annual Meeting & Exhibition Supplemental Proceedings (Springer, 2019). 413–420.

[21] J. Trzaska : Arch. Metall. Mater., (2016).

[22] K. Ishida : Metall. Mater. Trans. A, 48 (2017) 4990–4998.

[23] R. M. Bruscato : in ASTM Conference, Miami, Florida (1987).

[24] W. E. Erwin, E. WE, K. JG : (1982).

[25] E. J. Czyryca et al.: Nav. Eng. J., 102 (1990) 63–82.

[26] T. Kasuya, N. Yurioka : Weld. JOURNAL-NEW YORK-, 72 (1993) 263-s.

[27] S. W. Thompson : Mater. Charact., 77 (2013) 89–98.

[28] S. K. Dhua, S. K. Sen : Mater. Sci. Eng. A, 528 (2011) 6356–6365.

[29] S. K. Das, S. Tarafder, A. K. Panda, S. Chatterjee, A. Mitra : Philos. Mag., 87 (2007) 5065–5078.

[30] M. J. Sohrabi, H. Mirzadeh, , M. S. Mehranpour, A. Heydarinia, R. Razi : Arch. Civ. Mech. Eng., 19 (2019) 1409–1418.

[31] A. Ghosh, B. Mishra, S. Das, S. Chatterjee : Mater. Sci. Eng. A, 374 (2004) 43–55.

[32] G. H. Majzoobi, A. H. Mahmoudi, S. Moradi : Eng. Fract. Mech., 158 (2016) 179–193.

[33] D. Chae, C. J. Young, D. M. Goto, D. A. Koss : Metall. Mater. Trans. A, 32 (2001) 2229–2237.